

# Accretion Disk Origin of Earth's Water

Luca Vattuone<sup>1</sup>, Marco Smerieri<sup>1</sup>, Letizia Savio<sup>2</sup>, Krishna Muralidharan<sup>3</sup>, Michael J. Drake<sup>4,\*</sup>, and Mario Rocca<sup>1</sup>

<sup>1</sup> *Dipartimento di Fisica dell'Università di Genova and IMEM-CNR Unità operativa di Genova, Via Dodecaneso 33, 16146 Genova, Italy*

<sup>2</sup> *IMEM-CNR Unità operativa di Genova, Via Dodecaneso 33, 16146 Genova, Italy*

<sup>3</sup> *Department of Materials Sciences and Engineering, University of Arizona, Tucson, AZ 85721, USA*

<sup>4</sup> *Lunar and Planetary Laboratory, University of Arizona, Tucson, AZ 85721, USA*

**The presence of water on the Earth is an enigma. It is generally agreed that it was too hot at 1 AU for hydrous minerals to be stable in the accretion disk. Thus, Earth's water is conventionally believed to be delivered by comets or wet asteroids after Earth formed. However, wet asteroids and comets have elemental and isotopic properties that are inconsistent with those of Earth<sup>1</sup>, limiting the amount of water derived from comets and wet asteroids. It was thus proposed that water was introduced during planet growth in the accretion disk in a form stable under high temperature conditions. This hypothesis is supported by the presence of water in the disks around young stars<sup>2</sup> and by numerical simulations of water adsorption on silicate grains under conditions corresponding to those in the accretion disk<sup>3,4</sup> which showed that molecular chemisorption of water on forsterite (Mg rich end member of olivine, one of the main constituent of the dust grains) might account for the formation of several Earth oceans<sup>4</sup>. Here we show both by numerical and laboratory experiments that water adsorbs dissociatively on the olivine {100} surface at the temperature (~500-1500 K<sup>5</sup>) and water pressure (~10<sup>-8</sup> bar<sup>6</sup>) expected for the accretion disk, leaving an OH adlayer that is stable at least up to 900 K. This high temperature stability may result in the formation of many Earth oceans, provided that a viable mechanism to produce water from hydroxyl exists.**

Adsorption has not been considered a viable delivery source of water due to the misconception that it only physisorbed to the mineral surfaces and consequently that it was not stable at the high temperatures characteristic of the accretion disk at 1 astronomical unit (AU). This view was recently questioned by computational investigations of water interaction with olivine surfaces<sup>3,4,7</sup> that indicate the occurrence of chemisorption with binding energies strong enough to ensure the stability of molecular water even at high temperatures ( $> 700$  K)<sup>4</sup>. This information was then used in conjunction with kinetic Monte Carlo simulations (KMC)<sup>8</sup> to predict the kinetics of water adsorption and to demonstrate that many Earth oceans could be delivered via molecular chemisorption alone. However, these studies neglected the possible occurrence of water dissociation, a process that we show dominates water - olivine interactions in laboratory experiments performed under controlled Ultra High Vacuum conditions, in agreement with more sophisticated atomistic-based numerical simulations.

Experiments were performed by dosing olivine surfaces with water using a supersonic molecular beam (SMB), seeding the SMB either with  $N_2$  or He and varying the nozzle temperature. This method allows attainment of kinetic energies varying from  $E=0.06$  to  $E=0.30$  eV, an interval spanning a large part of the velocity distribution at the temperatures of the accretion disk. Experiments were performed for both the polished and unpolished side of an olivine (100) sample prepared in situ by ion bombardment and annealing (see supplementary material). Temperature Programmed Desorption (TPD) was used to probe water adsorption on the polished side. For the non-polished surface, thanks to its higher reactivity, the more accurate retarded reflector method of King and Wells (KW, see supplementary material<sup>9,10</sup>) could be employed for the determination of the sticking probability,  $S$ . The unpolished side better mimics real olivine surfaces in the accretion disk.

In Fig. 1 we show TPD traces recorded after subsequent water exposures (600 s at  $E=0.30$  eV) on the polished face of the olivine crystal at 138 K. Since in preliminary experiments neither  $H_2O$  nor  $H_2$  desorption (indicative of the presence of adsorbed H) was detected in the range from 165 K to 900 K, the sample was prepared for subsequent doses by annealing it just above the end of the main desorption peak. It is apparent that subsequent doses yield decreasing desorption signals. We assign the TPD peak to the desorption of water multilayers since: a) its intensity does not saturate with exposure and, at least for the first doses, it is clearly of order zero; b) on the non polished side, where  $S$  is directly measurable, it does not saturate even for prolonged exposures (up to 2400 sec, not shown). After the fourth dose the surface is readily passivated since no further desorption occurs even when the sample is prepared by heating it to 900 K. Only sputtering with  $Ne^+$  ions and annealing to 850 K for several minutes to recover surface order could restore the initial reactivity. Similar experiments performed at lower kinetic energy of the impinging water molecules (0.06 eV) yielded similar results. Given the strong dependence of  $S$  on surface cleanliness, the water beam was used to check for the surface chemical state, which for an insulating sample is difficult to characterize, since electron beam based spectroscopies are useless and optical spectroscopies explore the region immediately below the surface thus preventing the observation of adsorbates at low coverage.

In Fig. 2 we compare the effect of doses performed at low crystal temperature on a clean surface and on a surface pre-exposed to water well above room temperature. As mentioned above,  $S$  is measured directly for the unpolished surface while, for the polished side, water adsorption is

monitored by performing TPD after dosing. It is apparent that at low temperature adsorption occurs on the clean surface (both polished or unpolished) but not on a surface that has been pre-dosed with water at high temperature. We note that complete passivation of the polished side did not occur during a 1800 s dose on a clean surface at 136 K, nor did it occur during subsequent desorption of the multilayer since, as shown in the inset, significant water desorption is still observed after a subsequent equivalent probe dose. Efficient passivation takes thus place only when the surface is exposed at temperatures as high as 560 K. In similar experiments performed on the unpolished side (for which the probe uptake we used was of only 20 s to compensate for the higher reactivity) the high temperature pre-dose causes a decrease of S from 0.2 to below experimental sensitivity, thus confirming our conclusion.

The surface coverage ( $\Theta$ ) is given by  $\Theta = \langle S \rangle \Phi \Delta t$ , where  $\langle S \rangle$  is the average sticking probability,  $\Phi$  the water flux and  $\Delta t$  the duration of the uptake. Since the water flux for the H<sub>2</sub>O/He beam is  $\sim 0.02$  ML/s, we estimate that for high temperature exposures,  $\langle S \rangle$  has to be larger than  $5 \times 10^{-4}$  for the polished surface and close to  $\sim 0.015$  for the unpolished side, i.e., higher but still lower than KW sensitivity<sup>9</sup>. The unpolished surface best mimics a real surface of olivine in the accretion disk. Its higher reactivity is not unexpected since it is known that surface corrugation may enhance the accommodation into the physisorption well<sup>11</sup>, and that under-coordinated sites can more easily lead to breaking of intra-molecular chemical bonds and to the formation of stronger bonds with the surface as seen by experiments for several substrates<sup>12</sup> as well as by simulations of defected forsterite<sup>13</sup>.

These experiments clearly indicate that:

- a) significant water uptake takes place when dosing at 138 K, a fact which can be attributed to multilayer adsorption
- b) when annealing, part of the water layer desorbs and part dissociates forming OH and H since the concentration of free sites, available for further water adsorption, decreases with increasing number of doses;
- c) the hydroxylated surface produced is stable up to at least 900 K since annealing up to this temperature cannot restore the reactivity.

Further support for the hypothesis of water dissociation comes from atomistic calculations of the dissociation energies for the sites given in Fig. 3. The results are summarized in Table I. The {100} surface, which is a primary cleavage plane of olivine, is an interesting system as the relaxed unhydrated surface lends itself to large molecular adsorption energies<sup>3</sup>. For {100} we identify 4 possible adsorption sites denoted by S1 to S4. S1 is fully coordinated, and does not promote dissociation. The S2 site is coordinated to three oxygen atoms, and is located 1.5 Å higher than S1. S3 is nested between two surface tetrahedra and is bonded to 4 oxygen atoms. S4 is also four-coordinated, with three oxygen atoms lying on the surface. Amongst the 4 sites, S2 yields the highest dissociation energy, corresponding to 348 KJ/mol, which can be attributed to the fact that it is the least coordinated cation as well as to the fact that it is located close to the surface and is extremely susceptible to hydroxylation. S3 and S4 also yield very high dissociation energy values of 322 KJ/mol and 290 KJ/mol, respectively. Note that molecular water can associatively bind to the {100} surface very strongly close to steps, with an energy of about 250-280 KJ/mol. Thus from a computational standpoint, one can assume that on {100}

both associative and dissociative adsorption can occur, though based on energetics dissociation is preferred.

These numerical results agree well with the experiments reported here, in which the dissociated state is found to be the most stable. Experiments show moreover that annealing a water layer deposited at 138 K as well as dosing at high surface temperature clearly promotes dissociation, implying that the activation energy barriers separating all such molecularly adsorbed states from the dissociated state(s) are lower than the barrier for molecular water desorption.

These experiments show that, under the conditions corresponding to the early stages of planetary accretion, the {100} surface undergoes therefore hydroxylation. Since water adsorbs dissociatively at accretion disk temperatures, the difference between the water partial pressure in our supersonic molecular beam ( $\sim 10^{-8}$  mbar) and the one in the accretion disk ( $10^{-8}$  bar) is irrelevant. Both experimental and computational investigations presented in this work confirm that dissociation of water on olivine surfaces is the dominant adsorption mechanism. Since the lower heat of adsorption of molecularly chemisorbed water could account<sup>4</sup> for the formation of a number of Earth oceans ranging from 1 to 17, even more water would be adsorbed because of the stronger adsorption energy of dissociative adsorption.

Terrestrial planets today have (or had) however H<sub>2</sub>O, not OH. Thus, there must be a chemical pathway that leads from hydroxyl to water during the formation of the terrestrial planets. Although we cannot conclusively establish the path, we can imagine at least three possibilities.

The first involves the presence of H<sub>2</sub> in the accretion disk as an obvious source of hydrogen to recombine with hydroxyl. Adsorption of H<sub>2</sub> onto olivine has only been studied at low temperatures<sup>14</sup> that are irrelevant to our experiments. However, our work, shows no desorption of H<sub>2</sub> between 160 and 900 K, and independent calculations<sup>15</sup> indicate that atomic hydrogen produced by water dissociation on olivine is too weakly bonded ( $E_{\text{ads}} \sim 102$  kJ/mol) to remain on the surface at the temperatures of the accretion disk, thus ruling out recombinative desorption as a source of water.

A second hydrogen source is represented by the protons from the solar wind which could either react directly to form water or be implanted at high energies into olivine and recombine with hydroxyl to give water after the olivine has been accreted into planets and the planets start to melt due to the release of gravitational potential energy. Direct reaction is energetically plausible since it is well known that reaction of gas phase atomic hydrogen with adsorbed OH is strongly exothermic (by 511 kJ/mol) and barrierless<sup>15</sup>. Reaction in a magma ocean environment will occur late in the accretion of planets as they melt repeatedly. It is unfortunately yet unclear whether an adequate amount of hydrogen can impact or be implanted to quantitatively account for the water budget of the Earth, the only planet for which there is a reasonable estimate of water content.

Thirdly, recombination of OH with OH to form H<sub>2</sub>O and liberate oxygen in planetary magma oceans has not been studied. Since the process is exothermic by about 66 kJ/mol in the gas phase<sup>16</sup> and since the surface-O and surface-OH binding energies are similar, adsorption of OH in the accretion disk could account for both the water content of the terrestrial planets like Earth, and the relatively oxidized state of the silicate mantles.

Elkins-Tanton <sup>17</sup> shows that, once water is dissolved in a magma ocean, it outgasses within 10 million years to produce either a liquid water ocean, or a steam atmosphere that collapses into a water ocean, depending on the water content of the magma ocean. Thus, if water in the accretion disk is adsorbed onto grains as hydroxyls, it seems inevitable that oceans will exist on Earth and other rocky planets in our solar system and others within 10 million years of the end of accretion.

### *Acknowledgements*

This work was supported by NASA grants NNX07A1529 and NNX10AH09G and by PRIN MIUR 208 contract 020302002008.

### **References**

1. Drake, M.J. Origin of water in the terrestrial planets. *Meteoritics and Planetary Science* **40**, 519-527 (2005).
2. Bethell, T. & Bergin, E. Formation and survival of water in the Terrestrial planet forming region. *Science* **326**, 1675-1677 (2009).
3. Stimpfl, M., Walker, A.M., Drake, M.J., de Leeuw, N.H. & Deymier, P. An Ångstrom sized window on the origin of water in the inner solar system: atomistic simulation of adsorption of water on olivine. *Journal of Crystal Growth* **294**, 83-95 (2006).
4. Muralidharan, K., Deymier, P., Stimpfl, M., de Leeuw, N.H. & Drake, M.J. Origin of water in the inner solar system: a kinetic Monte Carlo study of water adsorption on forsterite. *Icarus* **198**, 400-407 (2008).
5. Boss, A.P., Temperatures in protoplanetary disks. *Ann. Rev. Earth Planet. Sci.* **26**, 53-80 (1998).
6. Lodders, K. Solar system abundances and condensation temperatures of the elements. *Astrophys. J.* **591** 1220- 1247 (2003).
7. de Leeuw, N.H. et al. Where on Earth has our water come from? *Chem. Comm.* **46**, 8923-8925 (2010).
8. Gillespie, D.T. Exact stochastic simulations of coupled chemical reactions. *J. Phys. Chem.* **81**, 2340-2361 (1977).
9. King, D.A. & Wells, M.G. Molecular beam investigation of adsorption kinetic on bulk metal targets, nitrogen on tungsten. *Surf. Sci.* **29**, 454-492 (1972).
10. Rocca, M., Valbusa, U., Gussoni, A., Maloberti, G. & Racca, L. Apparatus for adsorption studies. *Rev. Sci. Instr.* **62**, 2172-2176 (1991).
11. Weaver, J.F., Carlsson, A.F. & Madix, R.J. The adsorption and reaction of low molecular weight alkanes on metallic single crystal surfaces. *Surf. Sci. Rep.* **50**, 107-199 (2003).
12. Vattuone, L., Savio, L. & Rocca, M. Bridging the structure gap: chemistry of nanostructured surfaces at well defined defects. *Surf. Sci. Rep.* **63**, 101-168 (2008).

13. King, M.E. et al. Computer simulations of water interactions with low coordinated forsterite surface sites: implications for the origin of water in the inner solar system. *Earth Planet. Sci. Lett.* (2010) in press.
14. Vidali, G., Li, L., Roser, J.E. & Badman, R. Catalytic activity of interstellar grains: formation of molecular hydrogen on amorphous silicates. *Adv. Space Research* **43**, 1291-1298, (2009).
15. Goumans, T.P.M.; Catlow, C.R.A., Brown, W.A., Kastner, J. & Sherwood, P. An embedded cluster study of the formation of water on interstellar dust grains. *Phys. Chem. Chem Phys.* **11**, 5431-5436 (2009).
16. Deyerl, H.J., Clements, T.G., Luong, A.K. & Continetti, R.E., Transition state dynamics of the  $\text{OH} + \text{OH} \rightarrow \text{O} + \text{H}_2\text{O}$  reaction studied by dissociative photodetachment of  $\text{H}_2\text{O}_2^-$ . *J. Chem. Phys.* **115**, 6931-6940 (2001).
17. Elkins-Tanton, L.T. Formation of early water oceans on rocky planets. *Astrophys. Space Sci.* DOI 10.1007/s10509-010-0535-3 (2010).

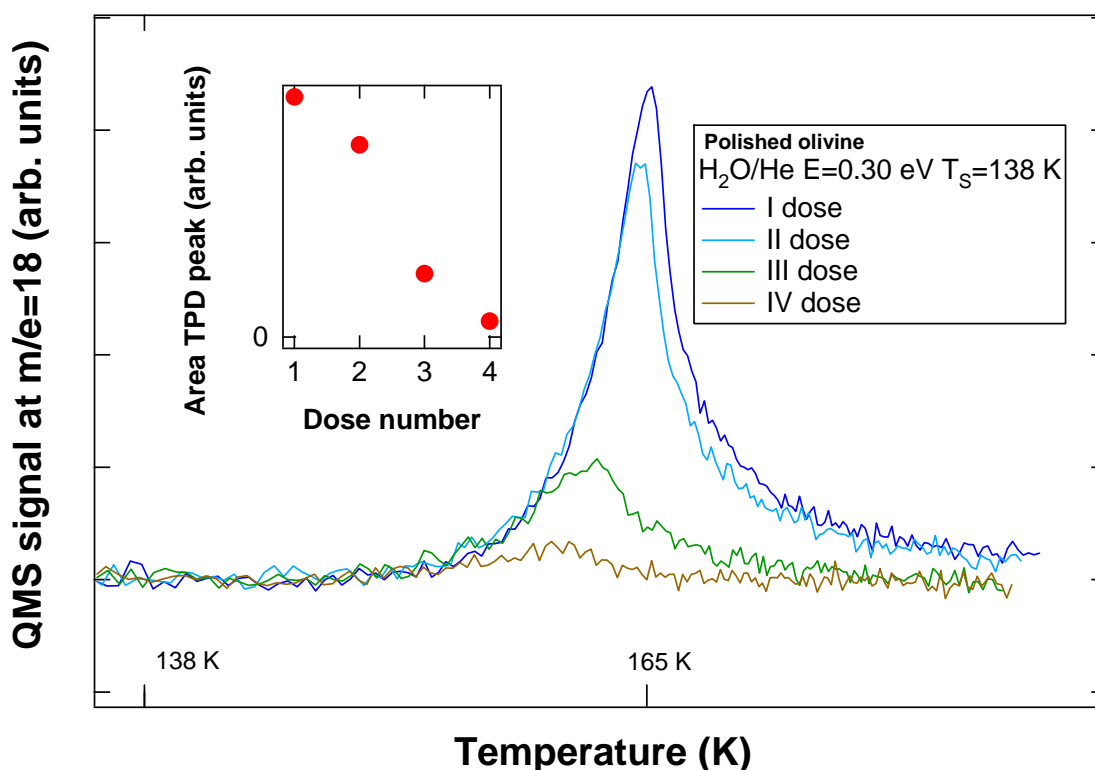
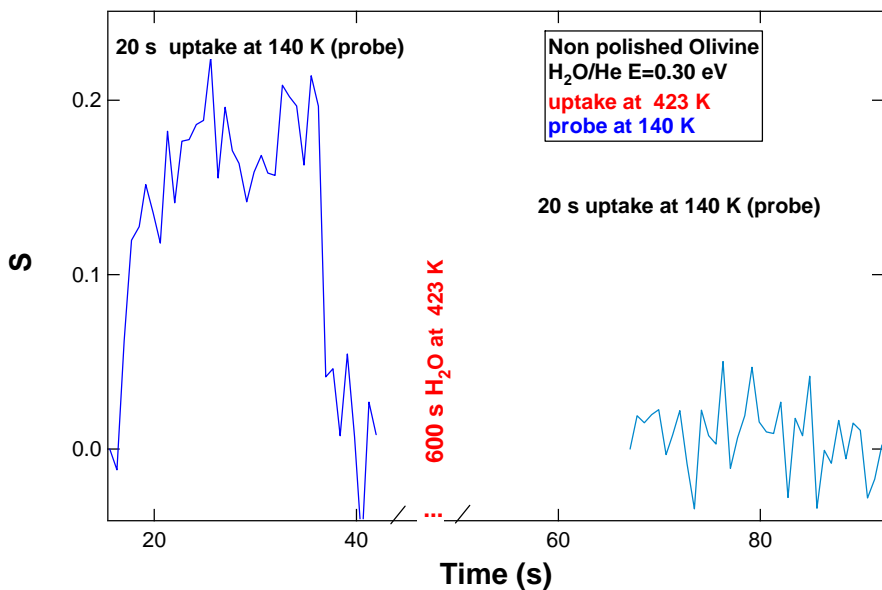
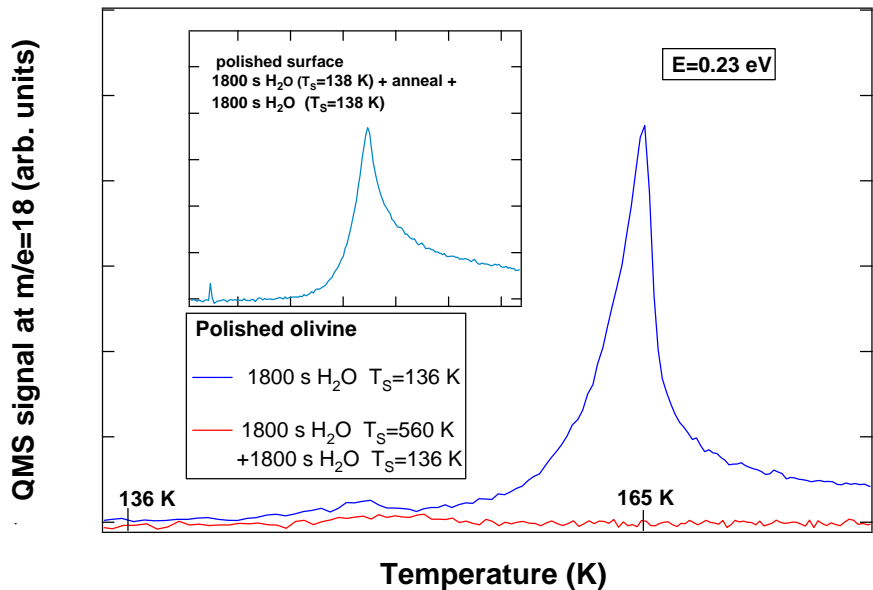


Figure 1 **Temperature Programmed Desorption (TPD) spectra from the {100} olivine surface for repeated identical doses (600 s) of water at 138 K.** The highest intensity peak corresponds to desorption of molecularly adsorbed water in multilayers. Prior to performing a new dose, the sample was prepared by heating the crystal well above the desorption temperature of molecularly adsorbed water (165 K). The lower signal observed for the subsequent doses

indicates gradual passivation of the surface. The inset shows the integrated desorption for the subsequent doses.



**Figure 2 Water adsorption on the polished (top) and on the non polished (bottom) side of the olivine sample.** Top: no water desorption is observed after the probe dose for a surface pre-exposed to water at 560 K. The inset shows the water desorption signal after a probe dose is given on a surface pre-exposed to water at 136 K and cleaned only by desorbing the multilayer. Bottom: subsequent exposures on an unpolished olivine surface. The first dose, performed at 140 K, shows a high adsorption probability ( $\sim 0.2$ ); the same dose performed under the identical conditions but for the sample pre-dosed for 600 s with water at 423 K shows that  $S$  is now below the sensitivity threshold.

### OLIVINE {100} SURFACE

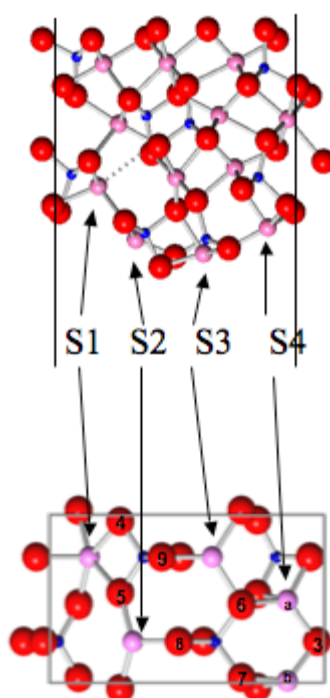


Figure 3 Illustrations of the {100} surface, where red, pink and blue represent oxygen, magnesium and silicon atoms respectively; the top illustration is a schematic representation of a part of the olivine slab viewed perpendicular to the surface (bottom side of the slab) and the bottom illustration represents view parallel to the surface unit cell. “Sn” identifies the possible adsorption sites, where “n” denotes the nth adsorption site.

| Surface | Adsorption site | $E_{mol}$ (kJ/mole) | $E_{diss}$ (kJ/mole) |
|---------|-----------------|---------------------|----------------------|
| {100}   | S1              | >-50                | -----                |
|         | S2              | -150                | -348.0               |
|         | S3              | -125                | -322.2               |
|         | S4              | -120                | -289.6               |

**Table 1 Molecular and Dissociative energies for forsterite {100} surface.**

## Supplementary Information.

### Experiments

The experimental apparatus is shown schematically in Fig. S1. It consists of an ultra high vacuum (UHV) chamber with a base pressure of  $10^{-10}$  mbar. The chamber is equipped with a supersonic molecular water-beam (SMB). A quadrupole mass spectrometer (QMS), which is not coaligned with the water-beam, measures the partial pressure of the gases in the UHV chamber. The local water pressure on the olivine surface with the water beam turned on is of the order  $10^{-8}$  mbar. The sample is mounted in a cage that may be cooled by liquid nitrogen fluxing and heated either radiatively or by electron bombardment. The temperature of the cage is measured by a chromel-alumel type thermocouple. To avoid possible contamination the sample was not glued to the cage, although this implies a non-ideal thermal contact with the cage. The temperature readings during the annealing cycles were thus calibrated with respect to water multilayer desorption which typically occurs at 165 K for ice <sup>1</sup>.

The sample is an approximately 1 mm thick slab of natural Pakistani olivine (Fo<sub>90</sub>) cut from a single crystal parallel to {100} and polished on one side to 1 micron smoothness (see image in Fig. S1). Adsorption of water was investigated for polished and unpolished {100} faces over a range of temperatures from 140 to 560 K.

The surface was cleaned by sputtering with Ne<sup>+</sup> ions followed by annealing to 900 K. Annealing to temperatures higher than 900 K was not attempted even while cleaning the sample to avoid possible modifications in its surface composition (e.g. by oxidation of Fe<sup>2+</sup> to Fe<sup>3+</sup>).

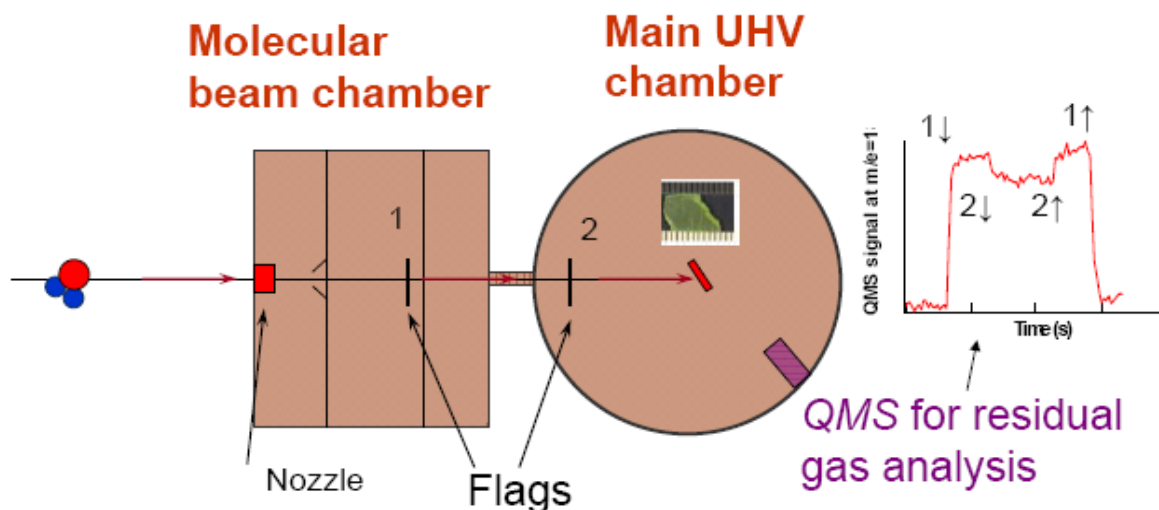


**Figure S1: Schematic drawing of the Supersonic Molecular beam chamber coupled to the ultra high vacuum chamber (Main UHV chamber).** The UHV chamber contains an olivine sample (see photo in the inset) and equipped with a quadrupole mass spectrometer (QMS) for residual gas analysis. The latter is used for King and Well's measurements of the sticking probability (see text).

The adsorption of water is measured by the retarded reflector method of King and Wells (KW)<sup>2</sup>, which has been successfully employed to examine adsorption of molecular species on different metallic<sup>3</sup> and oxide<sup>4</sup> surfaces. As our experimental results demonstrate, it can also be successfully used to study water adsorption on mineral surfaces. In this method, the partial pressure of water in the UHV chamber is recorded by the Quadrupole Mass Spectrometer (QMS) during exposure. During a typical experiment, the beam trajectory is first intercepted by an inert flag (1) located in the first chamber. Then flag 1 is removed and the beam is allowed to enter the UHV chamber. It is initially blocked by a second inert flag (2), resulting in an increase in the partial pressure to a value determined by the incoming flux and by the pumping speed. Then the second flag is removed and the beam strikes the sample. The diameter of the last collimator ensures that the spot of the supersonic molecular beam at the sample position is smaller than the sample itself thus ensuring a reliable measurement of the sticking probability at normal incidence. The position of impingement on the sample is checked optically by allowing a laser beam to pass through the same path travelled by the water molecules in the supersonic beam.

An abrupt decrease in partial pressure may be observed when the beam strikes the clean surface, corresponding to its gettering action, i.e., to the adsorption of water on the region of the olivine crystal seen by the supersonic molecular beam. The partial pressure tends eventually to its initial value when the surface is saturated with the probe gas and either adsorption stops (stable systems) or the rate of adsorption equals the one of desorption. In the latter case, when the beam is intercepted again by the inert flag (2), isothermal desorption is observed and the partial pressure shows a transient. The amount of adsorbed gas is derived by integrating the missing QMS signal versus time and multiplying by the beam flux, which needs therefore to be determined independently and often constitutes the principal source of systematical error. The sticking is only observable whenever it exceeds a few percent. At lower sticking percentages, Temperature Programmed Desorption (TPD) can characterize adsorption and the sticking probability can be determined from the ratio of desorbed gas and exposure.

## Calculations

Adsorption is a molecular/atomic-scale process and therefore requires an accurate description of the interatomic forces between the constituent particles (atoms and molecules). Traditional approaches towards modelling the interatomic interactions have relied upon parameterizations that can reproduce a host of thermodynamic properties of the systems under study. A relevant example of robust interatomic force-field models that have been successfully parameterized to model interactions in olivine and water are the suite of potentials derived by (i) Lewis and Catlow<sup>5</sup> for MgO and FeO, (ii) Sanders et al. for SiO<sub>2</sub><sup>6</sup>, and (iii) Baram and Parker for dissociated water<sup>7</sup>, respectively. We use the above potentials in our work to examine water dissociation and adsorption on forsterite (Mg end-member of olivine) surfaces in similar fashion to Stimpfl *et al.*<sup>8</sup>.

In order to create the different surfaces, the bulk crystal is numerically cleaved, in such a way that the SiO<sub>4</sub> groups are left intact, while only the Mg-O bonds are broken<sup>9</sup>. The respective bulk structures (i.e., atom coordinates and cell dimension) were based on the experimental work of Fujino *et al.*<sup>10</sup> and Kudoh *et al.*<sup>11</sup>. Further, the anhydrous surfaces are prepared such that

they are non-dipolar. To study dissociation energetics, it is assumed that -H coordinates with an underbonded surface oxygen atom, while -OH coordinates to a surface Mg cation. In this study, we examine the {100}, {010} and the {110} surfaces for both olivine end-members, and calculate the hydration energy ( $E_{diss}$ ) for the dissociation of a single water molecule, according to Eqn. 1,

$$E_{diss} = E_{hyd} - (E_{uhyd} + E_W) \quad (1)$$

where  $E_{hyd}$ ,  $E_{uhyd}$ , and  $E_W$  are the hydrated surface energy, energy of the unhydrated surface and cohesive energy of a single water molecule respectively.

### Additional bibliography

1. Hodgson, A. & Haq, S. Water adsorption and the wetting of metal surfaces. *Surf. Sci. Rep.* **64**, 381-451 (2009).
2. King, D.A. & Wells, M.G. Molecular beam investigation of adsorption kinetic on bulk metal targets, nitrogen on tungsten. *Surf. Sci.* **29**, 454-492 (1972).
3. Vattuone, L., Savio, L. & Rocca, M. Bridging the structure gap: chemistry of nanostructured surfaces at well defined defects. *Surf. Sci. Rep.* **63**, 101-168 (2008).
4. Funk, S., Hokkanen, B., Burghaus, U., Ghicov, A. & Schumuki, P. Unexpected adsorption of oxygen on TiO<sub>2</sub> nanotube arrays: influence of crystal structure. *Nano Letters*, **7**, 1091-1094 (2007).
5. Lewis, G.V. & Catlow, C.R.A. Potential models for ionic oxides. *J. Phys. C: Solid State Phys.* **18**, 1149-1161 (1985).
6. Sanders, M. J., Leslie, M. & Catlow, C.R.A. Interatomic potentials for SiO<sub>2</sub>. *J. Chem. Soc. Chem. Commun.*, **19**, 1271-1273 (1984)
7. de Leeuw, N:H. & Parker, S.C. Molecular-dynamics simulation of MgO surfaces in liquid water using a shell-model potential for water. *Phys. Rev. B* **58**, 13901-13908 (1998).
8. Stimpfl, M., Walker, A.M., Drake, M.J., de Leeuw, N.H. & Deymier, P. An angstrom sized window on the origin of water in the inner solar system: atomistic simulation of adsorption of water on olivine. *Journal of Crystal Growth* **294**, 83-95 (2006).
9. de Leeuw, N.H., Parker, S.C., Catlow, C.R.A. & Price, G.D. Modelling the effect of water on the surface structure and stability of forsterite. *Phys. Chem. Miner.* **27**(5), 332-341 (2000).
10. Fujino, K., Sasaki, S., Takeuchi, Y. & Sadanaga, R. X-ray determination of electron distributions in forsterite, fayalite and tephroite. *Acta Crystall.* **B37**, 513-518 (1981).
11. Kudoh, Y. & Takeda, H. Single crystal X-ray diffraction study on the bond compressibility of fayalite, Fe<sub>2</sub>SiO<sub>4</sub> and rutile, TiO<sub>2</sub> under high pressure. *Physica B+C*, **139**, 333-336 (1986).